ADVANCING EARTH AND SPACE SCIENCES

Earth and Space Science

RESEARCH ARTICLE
10.1029/2024EA004104

Special Collection:
Science from the Surface Water and Ocean Topography Satellite Mission

Evaluating Water Levels From the Surface Water and Ocean Topography (SWOT) Mission in a Hyper-Tidal Coastal and Estuarine Environment

I. D. Lichtman[1], P. S. Bell[1], C. Gommenginger[1], C. Banks[1], F. M. Calafat[2], J. Brown[1], and S. D. P. Williams[1]

[1]National Oceanography Centre, Southampton, UK, [2]University of the Balearic Islands, Palma, Spain

Key Points:

- Surface Water and Ocean Topography (SWOT) reveals complex, fast-changing 2D spatial patterns in water levels across the Land-Ocean Aquatic Continuum from rivers to the open sea
- SWOT water levels exhibit low errors, comparable to CryoSat-2, with a Root Mean Square Difference of 0.14 m against in-situ gauges
- Variation of elevation difference, between altimeter and water level gauges, with water elevation allowed correction for nearshore effects

Supporting Information:

Supporting Information may be found in the online version of this article.

Correspondence to:

I. D. Lichtman,
doulich@noc.ac.uk

Citation:

Lichtman, I. D., Bell, P. S., Gommenginger, C., Banks, C., Calafat, F. M., Brown, J., & Williams, S. D. P. (2025). Evaluating water levels from the surface water and ocean topography (SWOT) mission in a hyper-tidal coastal and estuarine environment. *Earth and Space Science*, *12*, e2024EA004104. https://doi.org/10.1029/2024EA004104

Received 19 NOV 2024
Accepted 5 JUN 2025

Author Contributions:

Conceptualization: I. D. Lichtman, P. S. Bell, C. Gommenginger, C. Banks, F. M. Calafat, J. Brown
Data curation: I. D. Lichtman, C. Banks
Formal analysis: I. D. Lichtman, P. S. Bell, C. Gommenginger, C. Banks, S. D. P. Williams
Funding acquisition: C. Gommenginger

Abstract The launch of the Surface Water and Ocean Topography (SWOT) satellite in December 2022 started a new era of swath altimetry, introducing an unprecedented global data set of high-resolution two-dimensional water level imagery. During its initial calibration and validation phase (cal/val), SWOT conducted daily observations for 3 months providing unparalleled insights into the high variability of water levels at daily and kilometer scales, far surpassing capabilities of past and current altimeters. Here, this novel data set is evaluated in the hyper-tidal coastal-estuarine environment of the Bristol Channel-Severn Estuary. SWOT total water levels (TWLs) are assessed against data from a network of in-situ water level gauges (WLGs) and compared to the performance of the CryoSat-2 satellite altimeter. In this region, CryoSat-2 water levels agree well with WLG data, with a Root Mean Square Difference (RMSD) of 0.17 m. Comparisons of SWOT Level 3 low rate 2 km (L3) total water level with WLG data reveal constant offsets that scale with water elevation, attributed to the spatial difference between the measurements. Once corrected, L3 TWLs achieve RMSDs ranging from 0.059 to 0.150 m against individual gauges. Overall, the scaled L3 data exhibit an RMSD of 0.137 m, a regression slope of 0.99 and offset +0.044 m, demonstrating that SWOT delivers high-quality water level data in these dynamic and challenging environments. SWOT's altimetry images reveal complex, changing spatial patterns across the Land-Ocean Aquatic Continuum. These daily measurements resolve fast-changing processes, such as river discharge events, sandbank movements and storm surges — phenomena missed by the 21-day cycle of the SWOT science phase.

Plain Language Summary Knowledge of water level at the coast and in rivers is vital for flood resilience in a changing global climate. Satellite measurements of water levels close to the coast have greater uncertainty, because of rivers and intertidal areas. At present, satellite measurements are monthly repeat 1D tracks validated at ocean scales of 60–200 km using tide gauges, unevenly distributed around coastlines. Nearshore dynamics add to the uncertainty in the comparison of the gauges and satellite. This means there are sparse spatial measurements, with high uncertainty, of water levels in coastal areas for most of the world. SWOT produces 2D maps of water level for 90% of the world enabling the assessment of water levels on a global scale. This work validates the SWOT data in one of the most globally complex coastal zones, the Bristol Channel and Severn River-Estuary. This area was selected as there is an extreme range of tide, storm surges and complex coastal geomorphology, with a network of water level gauges providing local observations, to get the best range of measurements possible. SWOT is returning high quality data in this challenging environment and clearly shows spatial patterns in water level from river, through estuary, to sea.

1. Introduction

Knowledge of water level and its accuracy at the coast and in rivers is vital for flood resilience and management of water resources in a changing global climate (Laignel et al., 2023; Lyddon et al., 2023; Rulent et al., 2020, 2021; Vignudelli et al., 2019; Woodworth et al., 2019). Few countries have comprehensive WLG networks, and these spatially sparse data can be complemented by satellite measurements though existing altimeters have widely spaced tracks providing low temporal and spatial resolution (Cazenave et al., 2022; Hart-Davis et al., 2024; Monahan et al., 2025a; Rulent et al., 2020). Tidal models can be used to provide water level estimates and predictions at high temporal and spatial resolution, but do not account for sea-level changes associated with land-ice melting and rely on calibration and validation data from water level gauges and satellites (e.g., Rulent et al., 2020). These models have reduced accuracy in regions of complex marine dynamics, such as near the coast

Methodology: I. D. Lichtman, P. S. Bell, C. Gommenginger, C. Banks, F. M. Calafat, J. Brown, S. D. P. Williams
Project administration: P. S. Bell, C. Gommenginger
Software: I. D. Lichtman, P. S. Bell
Writing – original draft: I. D. Lichtman, P. S. Bell, C. Gommenginger, S. D. P. Williams
Writing – review & editing: I. D. Lichtman, P. S. Bell, C. Gommenginger, C. Banks, F. M. Calafat, J. Brown, S. D. P. Williams

(Gregg et al., 2024; Hart-Davis et al., 2024), and where long term in-situ data are sparse (Ray et al., 2011; Rulent et al., 2020) and where rivers, surge and waves interactively add to the water elevation (e.g., Lyddon et al., 2020). 2D swath altimetry, with high spatial resolution, solves the problem of sparse measurements from water level gauges and conventional altimetry (Hart-Davis et al., 2024). Although 2D altimetry cannot resolve high-frequency variations, such as tides and storm surges, these features can be resolved spatially when coinciding with satellite overpasses, allowing their form and extent to be studied (Hart-Davis et al., 2024; Monahan et al., 2025a, 2025b).

The Surface Water and Ocean Topography (SWOT) mission is the first of its kind in satellite remote sensing, a swath altimeter producing 2D maps of marine and inland water levels globally (Fu et al., 2009, 2024). The SWOT KaRIn instrument, a Ka band radar interferometer, was designed to resolve from high vertical accuracy over oceans to high spatial resolution for freshwater bodies on land (Fu et al., 2009, 2024). Although not specifically designed for measuring coastal processes, these new data products will allow for a better understanding of processes at the coast including tides, sea level and storm surge (Laignel et al., 2023).

To validate the SWOT data for total water level (TWL), a set of WLG and CryoSat-2 data has been gathered, in Bristol Channel and Severn River-Estuary (BCSRE), during the 3-month daily repeat cal/val mission phase (31 March–10 July 2023). In addition, this work highlights issues of how the coastal dynamics, hydrology and morphology affect the comparison of satellite altimetry and WLGs, and how these features may be seen in the 2D SWOT data. Satellite measurements of water level close to the coast have greater uncertainty because of land and intertidal areas. This test case in an extreme environment aimed to get the largest range of sea level variability as possible, but with global relevance and applicability. The work presented here forms part of the SWOT Science Team validation work in estuaries around the world, including the Baie des Veys, Elbe, Guayas, Komo, Raz Blanchard and St. Lawrence estuaries (www.swot-adac.org. SWOT AdAC Consortium, 2025).

Here we aim to explore the quality of SWOT data in the coastal zone and rivers. For the UK contribution to the international SWOT Science Team validation work, the SWOT-UK project carried out a comprehensive program of campaigns and multidisciplinary research to:

- Explore uncertainties of existing satellite altimeters compared to water level gauges at the coast.
- Produce a validation scheme for the SWOT satellite data for TWL.
- Examine features of coastal dynamics expected to be resolved by SWOT data.

1.1. The Surface Water and Ocean Topography (SWOT) Mission

SWOT was launched 16 December 2022 to collect 2D maps of marine and terrestrial water level, the first for a satellite instrument. SWOT's KaRIn (Ka-band radar Interferometer) instrument has two 50 km swaths, either side of a Poseidon 3C nadir altimeter. The data are processed for high rate/high spatial resolution water level products intended for coastal and inshore waters and a low rate/high vertical accuracy product for oceans (Fu et al., 2009; Laignel et al., 2015). After commissioning, SWOT entered a three-month period of calibration and validation (cal/val) with daily repeat measurements over a set of 14 orbits (from April–July 2023. AVISO, 2024a). The operational phase of SWOT is a 21-day repeat orbit, with cross-over areas of ascending and descending passes covered 2–4 times during this period (AVISO, 2024a; Laignel et al., 2015). These novel data represent the cutting edge of satellite altimetry for the observation and study of the world's marine and freshwater water system and will provide data for calculating a global water level budget.

The KaRIn Level 2 Low-Rate products (L2 LR) were designed for ocean surfaces (AVISO, 2024b; JPL, 2023). The Basic and Expert products are grided to 2 km posting and resolution on a swath-aligned geographically fixed grid (AVISO, 2024b; JPL, 2023). The L3 products contain both KaRIn swath and Poseidon altimeter data combined into a single data set, with the best corrections available and multi-mission calibration (AVISO, 2025). Here, the L3 LR Expert v2.0.1 (Baseline C) 2 km product (Pass 016, cycles 476–577) is used for the main part of this work (AVISO, 2024c).

1.2. The Bristol Channel and Severn River-Estuary

On the west coast of the UK, the BCSRE, has several large urban areas and contains key port and power infrastructure. Since antiquity, this area has been a hub for maritime trade between the Mediterranean, Europe and beyond (Cunliffe, 2001). The BCSRE is highly dynamic with one of the largest tidal ranges in the world (~14 m),

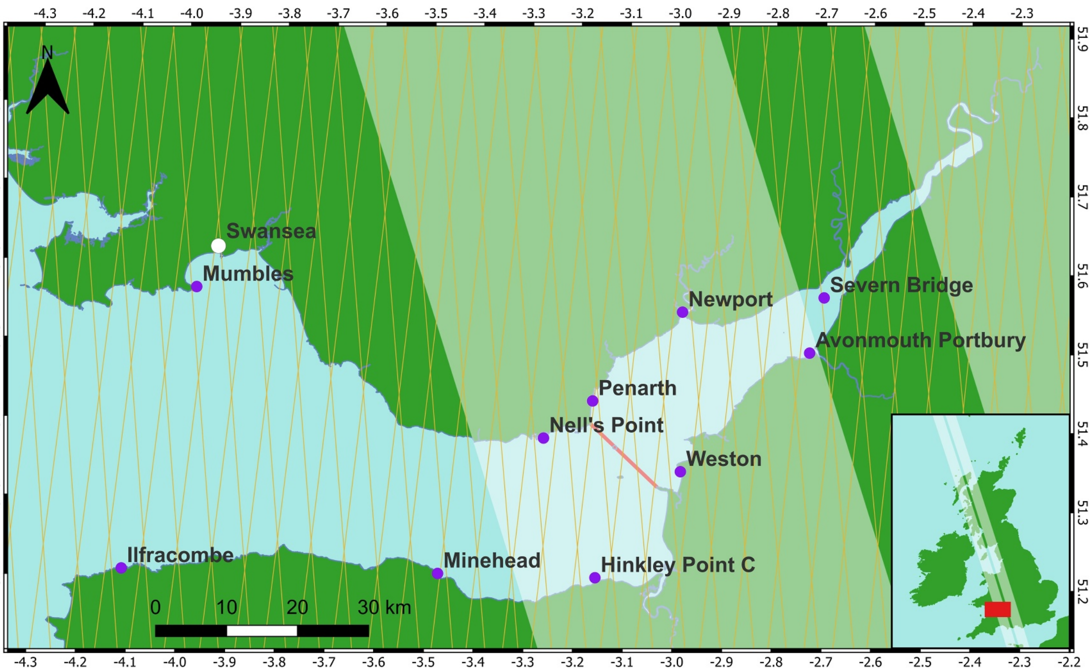

Figure 1. Map of the Bristol Channel and Severn Estuary area, UK, showing the water level gauge sites used in this study (purple circles). The red line marks the boundary between the Bristol Channel to the west and the Severn Estuary to the East. The surface water and ocean topography KaRIn swaths are shown in transparent white. The CryoSat-2 tracks are shown in orange. Swansea and Newport are the sites of the GNSS stations used for the vertical land movement estimate. The inset shows the location of the study area in the UK. (Contains Ordnance Survey data © Crown copyright and database right, 2023).

creating a vast intertidal area, along with strong currents and a tidal bore in the upper reaches (Archer, 2013; Dyer, 1984; Falconer et al., 2009; Gao & Adcock, 2017; Uncles, 2010). The flood risk due to tide and surge is magnified up estuary due to the morphology (Lyddon et al., 2018). In 1607CE a storm surge in this area caused the greatest loss of life due to a natural hazard in the UK for the past 500 years (Horsburgh & Horritt, 2006; Risk Management Solutions, 2007). The River Severn is the longest river in the UK with the second largest mean flow. The River Wye, the UK river with the sixth largest flow, also empties into the Severn Estuary (Natural Resources Wales, 1996). Waves can reach over 7 m at the western limit but are small upriver (Dhoop, 2019). In the Bristol Channel, the tide circulates as a Kelvin (coastal trapped) wave, causing cross-channel slopes (Uncles, 1984). In addition, the area has highly mobile sedimentary bedforms ranging from mud ridges to gravel waves and dunes (Carling et al., 2006; Dyer, 1984).

Due to this significance and complexity, the coastline surrounding these waters and upriver is covered by a network of water level gauges (WLGs) that has been continuously operational for a period of decades (Figure 1). The BCSRE is orientated east-west, with near perpendicular crossing of satellite tracks giving good quality data near to the shore. This makes it an ideal area for the validation of new satellite altimetry sensors.

1.3. Satellite SAR Altimetry

Synthetic Aperture Radar (SAR) altimeters improve the along track resolution, compared to standard altimeters, by using the delay-doppler method. This makes these measurements more suitable for coastal studies. CryoSat-2 (C2), a SAR altimeter, was designed to measure ice thickness, but also measures water level. Launched in 2010, it has now been operational for over 13 years. C2's main instrument is the Siral a Ku-band altimeter/interferometer. The orbit has a long repeat of ~369 days but has a 30-day sub cycle, and this allows greater coverage of the Earth's surface. C2 has a maximum resolution of 380 m along-track and 1.65 km across track, which gives ~7 km along-track resolution for the 1 Hz product (European Space Agency, 2021).

Table 1
List of Expected Sources and Estimates of Uncertainty for Coastal Altimetry Measurements in the Study Area

Source	Estimate of uncertainty
Orbit	~1 cm (Esteban-Fernandez, 2017)
Water level gauge leveling and structure motion	0.1 m (Ordnance survey, 2023a)
Geoid accuracy	5–10 cm (Pavlis et al., 2012)
Coastal and nearshore processes due to shallow water, waves, wind, coastal trapped tidal waves, intertidal areas, and river outflow	Up to tens of cm (Abessolo et al., 2023; Woodworth et al., 2019)
Dry and wet tropospheric atmospheric corrections	A few cm to tens of cm (Andersen & Scharroo, 2011)
Sea state bias correction, based on wave and wind data from altimeter or models, and with an algorithm not tuned to coastal areas	Should be a few cm, as waves are small in the study area (Andersen & Scharroo, 2011; Dhoop, 2019)
Vertical land movement effect on WLGs	Intra-annual variation and long-term trend is about 1 cm over 10 years in the study area
Residual error in spacecraft attitude, baseline length and phase drift	A few cm (Esteban-Fernandez, 2017; Surface Water and Ocean Topography Project, 2024)
Motion of the water currents and waves	<1 cm (Esteban-Fernandez, 2017)

1.4. Water Level Gauges

To support flood warning services, the UK has a network of Water Level Gauges (WLGs) and river gauges, measuring every 10 or 15 min, operated by a collaboration of the UK Environment Agency and regional partners. Additional in-situ Global Navigation Satellite Systems Interferometric Reflectometry (GNSS-IR) WLGs (Geremia-Nievinski et al., 2020; Larson et al., 2017; Williams & Nievinski, 2017, 2020), using the interference between the direct and reflected navigation signals, were deployed to fill gaps in the existing WLG network. The benefit of the GNSS-IR WLGs is that they are low-cost and easy to deploy compared with conventional gauges. Some of the WLGs are of unknown leveling quality and this work will help identify problematic gauges using the altimetry data.

1.5. Sources of Uncertainty in Water Level Measurements

Satellite measurements close to the coast have been considered noisier than in the open ocean (Cipollini et al., 2017). While this is largely because of waveform contamination by the presence of land in the altimeter footprint, it may also be partly due to effects in shallow waters from wave shoaling, set up and set down influencing altimetry measurements (Abessolo et al., 2023). In addition to this, in enclosed bays or estuaries, cross-channel slopes can be caused by trapped tidal waves. A list of expected sources of uncertainty their estimates is given in Table 1.

The orbital tracks of the satellites do not pass directly over the WLGs in the study area. This offset between WLG and altimeter measurement results in uncertainty due to water surface slope, from differences in tidal phase, circulation, river flow, intertidal wetting and drying, and coastal processes (Abessolo et al., 2023; Hart-Davis et al., 2024; Woodworth et al., 2019). Wave set-up and set-down can result in sea level variation, depending on the bathymetry and coastal geomorphology, over monthly, seasonal and interannual periods (Abessolo et al., 2023; Woodworth et al., 2019). Intertidal areas can remain wet after the tide has gone out, returning backscatter signal, and the level of uncertainty will depend on tidal range and bathymetry.

The travel time of the altimeter radar pulse is affected by atmospheric conditions, and corrections for this rely on measurements and models. The dry tropospheric correction degrades toward the coast and wet tropospheric correction WTC is highly variable near the coast (Andersen & Scharroo, 2011).

Geoid data are used to align the elevation data from satellites and in-situ gauges. The EGM2008 geoid has a 1-min horizontal resolution, approximately 2 km, and a vertical accuracy of the order ±5–10 cm (Karney, 2013; Pavlis et al., 2012). In the area of interest, the geoid varies in the order of 1.5 m over 50 km.

Vertical Land Movement (VLM) has a small effect on the tide gauge water levels over the period of the altimetry observations (Blewitt et al., 2016; Gravelle et al., 2023; Hammond et al., 2021; Woodworth et al., 2019; Wöppelmann & Marcos, 2016). The Intra-annual variation and long-term trend at Newport has a range of Vertical Land Movement (VLM) of about 20 mm (2004–2009), and about 25 mm (2010–2021) at Swansea (Dow et al., 2009; SONEL, 2023, stations 4,320 and 3,255). VLM can be corrected in the WLG using data from GNSS stations in the area when comparing these data to the satellite altimetry data (Blewitt et al., 2016; Gravelle et al., 2023). However, as this is a small amount of uncertainty for the 3-month cal/val period compared to other sources (Table 1) and as the nearest GNSS station (Newport) was decommissioned in 2009, we have not corrected for VLM.

The providers of SWOT data are still undertaking improvements in the calibration and correction of their products. Improvements to the KaRIn height calibration will be applied in future releases, affecting height measurement ~1 cm (Surface Water and Ocean Topography Project, 2024). Slow temporal variations result in height errors in the KaRIn data ~1 cm and these are yet to be corrected (Surface Water and Ocean Topography Project, 2024). Errors due to the motion of the water (i.e., currents and waves) will also cause height errors, but these cannot be corrected (Esteban-Fernandez, 2017).

Systematic errors from residual spacecraft roll, change in antenna baseline length (thermal contraction and expansion) and phase drift between the two radar channels will cause height errors, but these are reduced using the crossover correction (Dibarboure et al., 2022; Esteban-Fernandez, 2017). Crossover correction uses ocean crossover areas, from the ascending and descending passes, to compare KaRIn measurements, which allows the estimation of some systematic errors (Dibarboure et al., 2022; Esteban-Fernandez, 2017). The variation in the vertical velocity of the spacecraft velocity can result in a slowly changing height error of up to 2.5 cm, though crossover correction could remove some of this effect (Surface Water and Ocean Topography Project, 2024).

The root-mean-square difference (RMSD) between the C2 data and tide gauges was found to be 0.07 m by Calafat et al. (2017) on a global scale, but for coastal sites in the UK the RMSD for altimetry can be as good as 0.04 m (Cipollini et al., 2017). As the gauge data and satellite altimetry data are not collocated, with most gauges located on the land where the altimeter does not have a clear area of water to observe, it is inevitable that there will be some differences between the measurements (Cipollini et al., 2017).

2. Methods

2.1. Data Sources

CryoSat 2 (C2) is novel in that its orbit repeats every 369 days with a 30-day sub orbit. This allows a greater spatial coverage than the widely spaced tracks of standard altimeters and for more WLG sites to be matched to passes. The C2 data used were the Geophysical Ocean Product (GOP) data downloaded from ftp://science-pds.cryosat.esa.int/ (Euroban Space Agency, 2024; Mertz et al., 2019) extracted for the period 1 January 2012–31 July 2023. The quality control process was defined in Calafat et al. (2017) and removes data based on flags and out of range values. GOP data have a latency of ~30 days and represent the best quality of C2 data with consolidated orbits. The C2 1 Hz product was chosen to match best with the 2 km resolution of the L3 SWOT product, with less scatter than the C2 20 Hz product. The C2 data are used show the expected fit and uncertainty of satellite altimetry data compared to WLG data (Section 3.1).

Due to the importance of the Bristol Channel and Severn estuary, this region has a dense distribution of WLGs that cover the full width of the western SWOT swath, ~60 km. Water level gauge data were retrieved using the Environment Agency Real Time flood-monitoring and Channel Coastal Observatory APIs (Channel Coastal Observatort, 2024; Environment Agency, 2024; Lichtman et al., 2024). These data provide the standard by which the SWOT and C2 data are evaluated, in Sections 3.2–3.5.

The SWOT L3 data product, merged L2 KaRIn and Poseidon nadir data, uses the state-of-the-art research-grade upgrades with the best corrections available and multi-mission calibration (AVISO, 2025). The SWOT data were downloaded from the AVISO FTP site (AVISO, 2024b, 2024c). The L3 LR Expert 2 km data product was selected as this is the standard oceanographic data product.

10.1029/2024EA004104

2.2. Correction of the Satellite Altimetry Data

Sea level in the SWOT L3 data set is given as sea surface height anomaly (SSHA), with corrections applied, and additional variables supplied to remove or add corrections as required to get the desired sea surface height (SSH) variable. For the C2, the SSH is derived from the range measurement and satellite altitude data, with applied corrections. Here the total water level (TWL) is used as the measure of SSH, the SSH uncorrected for water tide and atmospheric pressure effects, to be as close to the WLG measurements as possible. Both C2 and SWOT L3 data had the same corrections applied to derive TWL, though some of these were from different sources. The corrections in common to C2 and SWOT L3 were The Dry and Wet tropospheric correction - European Centre for Medium-Range Weather Forecasts (ECMWF) model; and Global Ionospheric Map (AVISO, 2025; European Space Agency, 2021). The C2 product uses an empirical correction proportional to the significant wave height (SWH) from the C2 data for the Sea State Bias|sea sate bias (SSB) correction, Solid earth tide correction is the Cartwright model/Cartwright and Edden tables, and Geocentric Polar Tide correction the instantaneous polar location (European Space Agency, 2021). The SWOT L3 product: SSB - an empirical correction proportional to the SWH from the SWOT data, Solid earth tide correction - Elastic response to tidal potential, Geocentric Polar Tide - Mean Pole Location (AVISO, 2025).

The satellite altimetry data were corrected for atmospheric transmission and geophysical effects (Andersen & Scharroo, 2011; Bonnefond et al., 2011). The WTC, dry tropospheric correction and ionospheric correction remove the effects of the atmosphere on the propagation speed of the radar pulse. The WLG data will include the effects of local atmospheric pressure and wind, so dynamic atmospheric correction (DAC) is not applied to remove these effects from the altimeter data (Pérez et al., 2012; Rulent et al., 2020). Sea state bias correction is included to remove the bias of the altimeter range measurement due to the troughs of water waves (Andersen & Scharroo, 2011).

Tidal forces from the Sun and Moon deform the Earth, and this effect is accounted for by the solid Earth tide correction. Movement of the Earth's rotational axis causes a long-period distortion of the crust, and this effect is accounted for by the polar tide correction. The SWOT data includes an additional correction for differences between ascending and descending passes, and systematic errors (crossover correction; see Section 1.5, above, for more details). As ocean tide models are inaccurate in the study area (Gregg et al., 2024; Hart-Davis et al., 2024), due to low spatial resolution and morphological effects, the altimetry and WLG data were not corrected for water tide. The Geocentric Ocean Tide Height correction has not been included as this corrects for the change in seabed height due to water loading by the tide. The internal tide correction has been removed as it does not affect our study area.

For C2, TWL was calculated from the range between the satellite and the water and the altitude of the satellite above the reference ellipsoid, with atmospheric and Earth tide corrections (Equation 1). For the SWOT L3 SSHA, ocean tide, mean sea surface, DAC were removed to derive TWL (Equation 2). By convention, range and geophysical corrections are applied by subtracting them from the SSH and removed by adding them (Andersen & Scharroo, 2011).

Algorithm for calculating TWL for Cryosat 2 data

$$\begin{aligned}\text{Corrected Range} &= \text{Range} + \text{Wet Tropospheric Correction} + \text{Dry Tropospheric Correction}\\&\quad + \text{Ionospheric Correction}\\\text{Total Water Level} &= \text{Altitude} - \text{Corrected Range–Solid Earth Tide} - \text{Pole Tide} - \text{Sea State Bias}\end{aligned} \tag{1}$$

Algorithm for calculating TWL for SWOT L3 data

$$\begin{aligned}\text{Total Water Level} &= \text{Sea Surface Height Anomaly} + \text{Ocean tide} + \text{Mean Sea Surface}\\&\quad + \text{Dynamic Atmospheric Correction}\end{aligned} \tag{2}$$

All the altimeter data were referenced to EGM2008 geoid using geographiclib v2.3.2 (WGS84 EGM2008, 1-min grid. http://earth-info.nga.mil/GandG/wgs84/gravitymod/egm2008. Karney, 2013; Pavlis et al., 2012), for comparison to the gauge data.

10.1029/2024EA004104

2.3. Filtering the Satellite Altimetry Data

The data were filtered for extreme values outside the expected range of tide and wave height and masked to remove land data. Quality flags have not been applied, as these are tuned for open ocean use and would remove most data near the coast (AVISO, 2025). As the SWOT data products are still very new, the corrections supplied with the SWOT data products are improving over time, and problems are routinely discovered and corrected. Details of corrections and issues in different product versions are found in the DUACS Level-3 SWOT KaRIn (L3_LR_SSH) User Handbook (AVISO, 2025) and in the product release notes (Surface Water and Ocean Topography Project, 2024).

The maximum tidal range in the Severn Estuary is about 14 m, with a variation of surge residual from −1.0 to 1.5 m for March–July 2023, at Avonmouth (National Tidal and Sea Level Facility, 2024a, 2024b). The highest skew surge recorded at Avonmouth was 1.95 m, on 24 February 1997 (National Tidal and Sea Level Facility, 2024c). Limits of −9 m and +9 m around the geoid level were used to remove outlier data points from the WLG and SSH data. Based on the 7.79 m SWH for a 50-year return period at Bideford Bay (Dhoop, 2019), in the Bristol Channel, a limit of 8 m was chosen as the largest expected SWH and used to filter the SSB correction data. Where the SSB correction was not available up estuary (upriver/east of 2.7°W), the maximum SSB value was used as waves are small in this area (Dhoop, 2019). The high-water line digital boundary from UK Office of National Statistics (Office for National Statistics, 2023) was used to create a shoreline mask, at one arc-second resolution (∼30 m), to remove data over land.

Each pass with more than two data points was filtered for spikes in SSH, with points greater than 3 times the median absolute deviation discarded. Altimetry data was selected using a 6 km radius around each WLG site, to allow for the offset of the C2 altimeter track. A median was taken from the SWOT data of each pass within the radius, of between 2 and 17 measurements, to reduce the effect of extreme values and water surface slope. The water surface slope is examined in Section 3.2, below.

2.4. Matching the Water Level Gauge and Satellite Altimetry Data

All the WLG data were converted from Ordnance Datum Newlyn to ETRS89/WGS 84 ellipsoid using a software utility provided by the Ordnance Survey (Michell, 2015; Ordnance survey, 2023b). All the locations of the sites have been checked and, where possible, the original WLG leveling reports were obtained. The datum for the Severn Bridge gauge was surveyed using the Ordnance Survey Geoid Model 2002 and the values were corrected to the current standard, OSGM15, using the Ordnance Survey software. When correcting the water level data from OSGM02 to OSGM15, for the Severn Bridge site, the offset was found to be 0.03 m. OSGM15 was used to survey the gauges at Penarth. However, for the other sites either the standard used was the National Leveling Network or the standard information was not available. The error between OSTN15 and the old triangulation network stations is 0.1 m RMS for the UK (Ordnance survey, 2023a). It is expected that the overall uncertainty in the WLG data due to leveling is in the order of 0.1 m. This will be seen as a fixed offset for each gauge site compared to the satellite data. All the WLG data were corrected to EGM2008 geoid for comparison (Karney, 2013; Pavlis et al., 2012).

As the times of the satellite passes do not exactly match the times of the 10 or 15-min WLG measurements, the WLG data were interpolated to the time points of the altimetry measurement. This was done using a two-hour window of WLG data and filtering for spikes greater than 3 times the median absolute deviation, before interpolation using a modified Akima algorithm (MATLAB interp1 function). The modified Akima algorithm works well for both oscillatory and flat regions in the data (Akima, 1970; Ionita, 2019; The MathWorks, Inc, 2022). This is necessary as some of the WLGs only measure part of the tidal curve, as they are in the intertidal zone or on a river.

To identify if the data matched points were on the flood or ebb tide, the gradient of the WLG data in the 2-hr window was determined and the median of these taken. This was done to assess differences between flood and ebb tide in the data.

The WLG sites that dried out at low water, only measuring part of a single high-low tidal cycle, were filtered for when the water was absent, defaulted to river or bed level, as the altimeter would still return offshore values. These sites were manually flagged in the metadata to identify those that needed filtering. To determine the level without tidal influence, where the WLG data flatlines, the top half the tide of a running 2-hr window of WLG data (above the mean) were removed. Then, a mode filter was used on the bottom half of the tide to determine the default level and altimeter points below this level were excluded.

Differences between the satellite and gauge data greater than a meter represent an error of an order of over 1,000% considering the gauge and satellite resolutions are of order centimeters. Satellite and gauge data matches with differences greater than one meter were removed from the data set used in the regression analysis.

Gauges clearly affected by river flow and local morphology, with all points scattered below the 1:1 line of the WLG-altimeter plots, were removed from the matching process. On plotting the individual gauges against the altimeter data, the effects of intertidal morphology and shallow water processes could be seen in the data (see results Section 3.4, below, for details). Outliers were removed from the SWOT KaRIn data by identifying differences between the altimeter and WLG data greater than 3 times the median absolute deviation, after the scaling slope with elevation had been removed (see Section 3.4 for more details on the scaling slope). This scaling effect could not be corrected in the C2 data, due to the small number of points for each individual WLG site.

2.5. Assessing the Spatial Sea Surface Features of the SWOT Data

As a qualitative check on the SWOT data, the L3 LR 2 km SSH was visually compared to the FES2022 tidal model output packaged with the L3 data (AVISO, 2024d). For the comparison, the SWOT L3 SSHA data were converted to SSH, removing the corrections for ocean tide and mean sea surface and leaving in the solid earth tide, pole tide and dynamic atmospheric effect corrections. Both L3 and FES2022 data sets were normalized (centered to mean of zero and scaled to one median absolute deviation) to match color scales as closely as possible. Some differences are expected, as the FES2022 model does not include storm surge, or fine scale bathymetry and coastal morphology. SWOT passes were selected for time points as close as possible to the state of tide at Hinkley Point C (Figure 1), for low water, mid-water flood, high water and midwater ebb.

To quantify the effect of water surface slope, along and across channel slope were looked separately. Along channel slope is expected as the tidal wave travels in and out of the BCSRE. In addition, the tide circulates as a Kelvin wave in the Bristol Channel, causing water surface slope across the channel (Uncles, 1984). The cross-channel slope is measured between Nell's point and Hinkley Point (inner Bristol Channel), as this runs near to parallel with the track of SWOT and is close to perpendicular to the channel. For the along channel slope, the nearest SWOT sample point to the mid-point between the two shores the along centerline of the BCSRE was taken (see Section 3.2 below).

3. Results

3.1. Spatial Variability in the SWOT L3 LR Expert Data Compared to the FES2022 Tidal Model

As a qualitative check on the spatial variability in the SWOT data, the L3 LR 2 km SSH was visually compared to the FES2022 tidal model (AVISO, 2024d). For low water and mid-water flood, the SWOT L3 LR and FES2022 data compare well (Figures 2a and 2b). At low water, exposed intertidal areas and sandbanks in the middle of the channel are seen as “high points” in the SWOT L3 data, along the coast and further up the estuary, but not in the FES2022 data (Figure 2a). At high water and mid-water ebb, the high water in FES2022 seems to lag behind SWOT (Figures 2c and 2d). This may be due to FES2022 not modeling the frictional effects due to shallow water and the presence of small islands at the boundary between the Bristol Channel and Severn Estuary (Figure 1, red line). The resolution of FES2022 at coastal scale is 2 km–500 m (AVISO, 2024d), which may not fully resolve the small islands at the boundary between the Bristol channel and Severn Estuary as they are less than 1 km long. Although data were missing from the study area for 78 out of the 97 SWOT cal/val passes, due to a problem with missing data in the reference surface used for the Level 1B processing of the latest SWOT product versions (SWOT Project, 2024), the patterns shown in Figure 2 were consistent throughout the available data. The full sequence of cal/val period can be found in the Video S1 Supporting Information S2.

3.2. Along and Cross Channel Water Surface Slope

For the SWOT passes used in Figure 2, at different states of tide, the along and cross channel slopes are shown in Figure 3. The cross-channel slope is measured between Nell's point and Hinkley Point, and for the along channel slope, the nearest SWOT sample point to the mid-point between the two shores is taken along the centerline (Figure 3a).

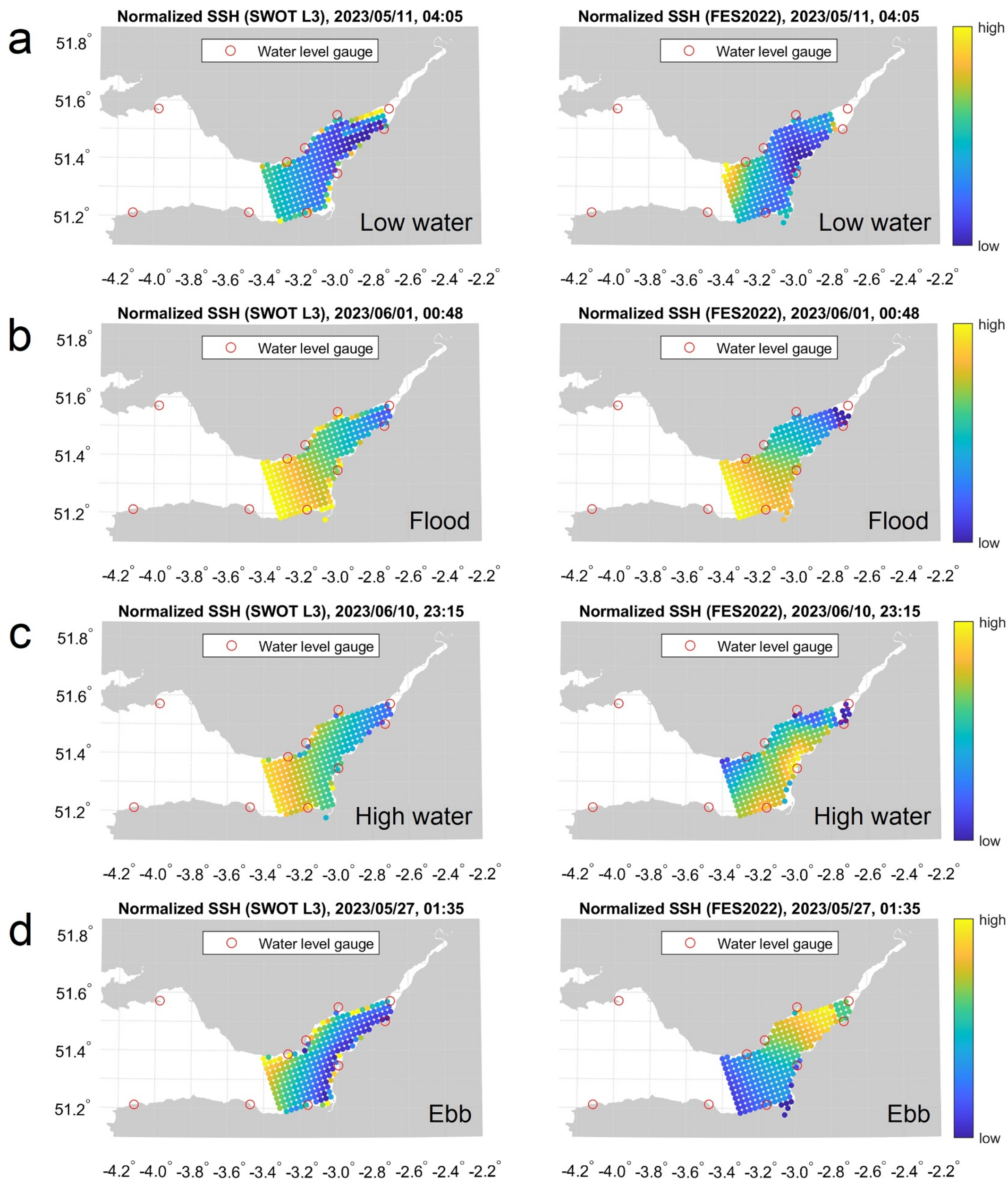

Figure 2. (left) Surface water and ocean topography L3 LR 2 km (v2.0.1) unedited sea surface height data and (right) FES2022 tidal model, shown for examples of different states of tide. For visual comparison data sets have been normalized to match the color scales. The states of tide were selected at Hinkley Point C for: (a) Low water, (b) Mid-water flood, (c) High water and (d) Mid-water ebb.

The steepest slopes occur around mid-tide. For all the available cal/val data, the mean cross-swath/track (along channel) slope is 0.016 m/km and the maximum is 0.038 m/km, and the mean along-swath/track (cross channel) slope is 0.008 m/km and the maximum is 0.027 m/km. A median filter can correct for the along channel slope, as there are data points upstream and downstream. However, as most of the WLGs are situated on the coastline the median is not able to compensate for the cross-channel slope, though as the effect of cross-channel slope is about half that of the along channel slope, this is less of a concern. Estimating from the cross-channel slope, an uncertainty of up to 0.08 m over 2 km is expected.

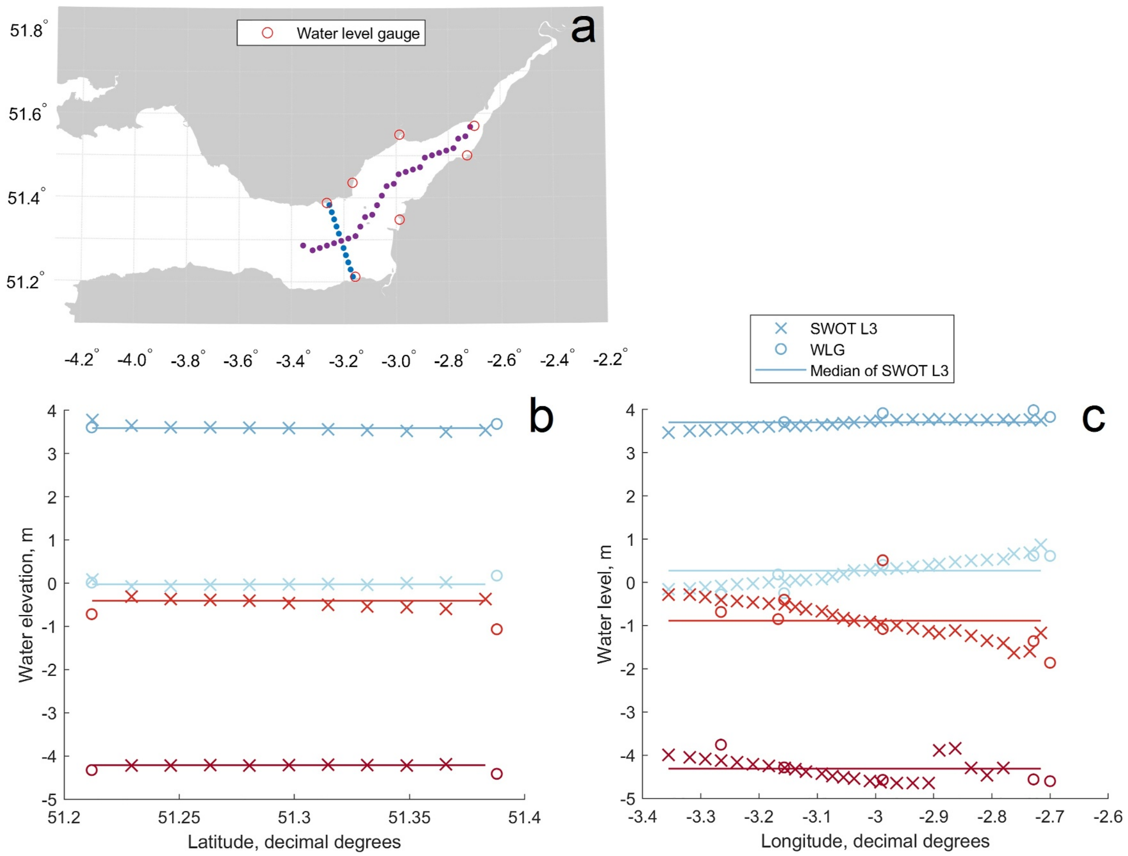

Figure 3. Surface water and ocean topography L3 LR 2 km (v2.0.1) water surface slope in the Bristol channel and severn river-estuary (BCSRE) (a) Map of the lines across channel and along the channel centerline, corresponding to the data show in panels (b and c). (b) Cross-channel slope between Nell's point and Hinkley Point C. (c) Along-channel slope along the centerline of the BCSRE. Data are for the states of tide at Hinkley Point C, from low to high elevation: Low water, Mid-water flood, Mid-water ebb and High water (see Figure 2).

3.3. Comparison of the CryoSat-2 1 Hz Data to Gauge Data

The C2 data were analyzed using data from all the WLGs shown in Figure 1, including sites outside the SWOT swath, for the period 1 January 2012–31 July 2023, to ensure a good number of measurements. Considering the uncertainties outlined in Section 1.5 above, the comparison of C2 data to the WLG data (Figure 4) is within a couple of tens of cm RMSD (0.165 m. Mean Absolute Error, MAE, 0.118 m) and close to the one-to-one line (the equivalent figure for the C2 20 Hz is shown in the Figure S1 Supporting Information S1). The linear regression slope is 0.97 and offset −0.007 m (Figure 4). The regression between C2 and WLG has an R^2 of 0.996, compared well with the C2 (1 Hz)-WLG correlation 0.80 of Rulent et al. (2020), for a selection of UK gauges. Overall, the WLG network is consistent compared to the altimetry data, despite not being corrected for nearshore processes and river input.

3.4. Effect of Coastal Morphology and Processes on Altimeter-Water Level Gauge Comparison

Van de Casteele diagrams are usually used to assess the quality of water level gauges by comparing them to a reference gauge (IOC, 1985; Martín Míguez et al., 2008). These diagrams are plots of the difference between two sources of water level against water height, showing the effect of variation between low and high water over a tidal cycle. For high quality, perfectly collocated measurements, a straight vertical line would be expected (IOC, 1985). A scaling problem would result in a slope, for all or part of the data, and can be due to the distance between water level measurements (IOC, 1985; Pérez et al., 2012). Within our study area, the tidal range changes significantly as the estuary narrows, increasing by over 1.5 m between Hinkley Point and Avonmouth. Thus, any slight positional offset between SWOT and tide gauge measurement points will almost certainly result in a scaling error. By comparing the SWOT altimetry data with individual water level gauges, within the SWOT swath

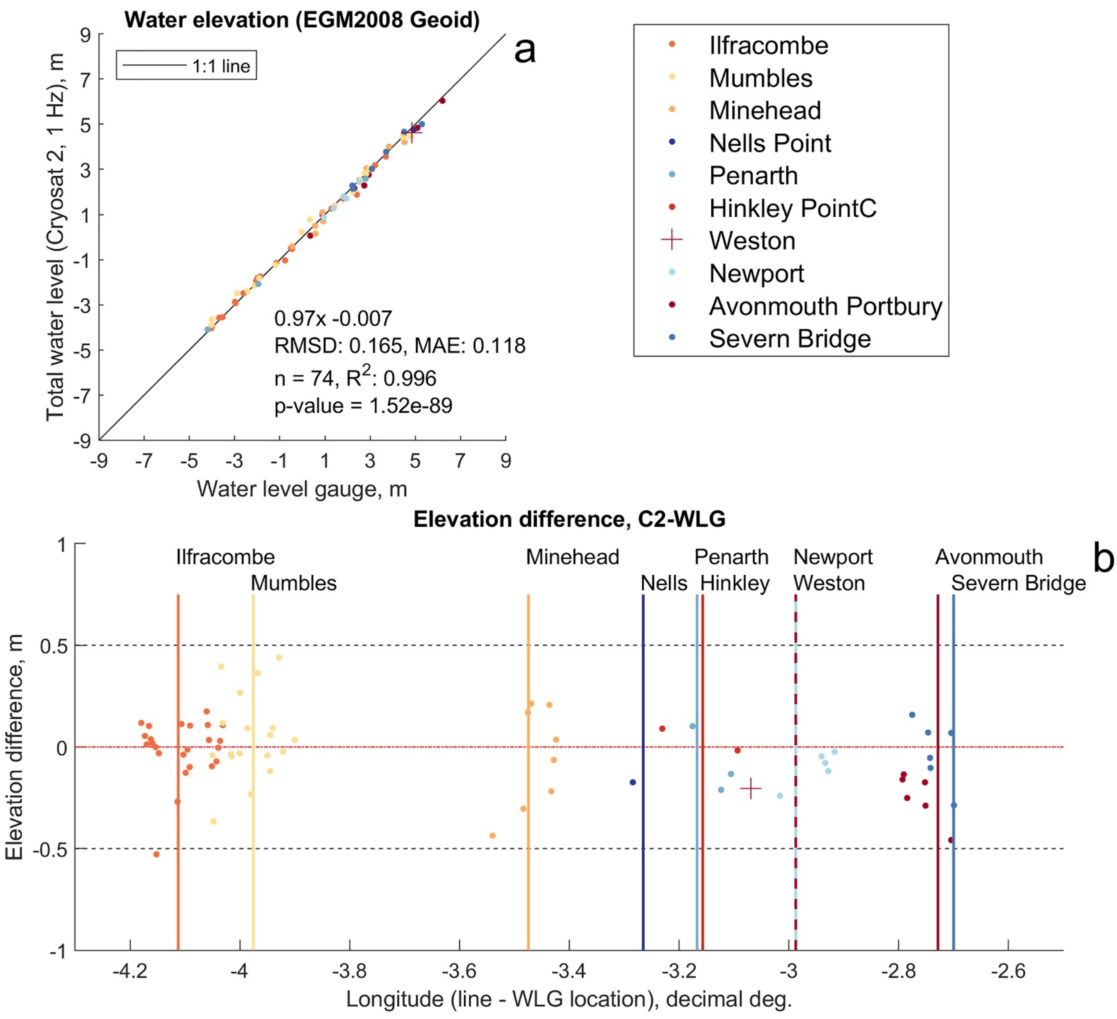

Figure 4. CryoSat-2 (C2) 1 Hz total water level (TWL), median for the 6 km radius around the water level gauges, against WLG (corrected to EMG2008 geoid). Data from 1 January 2012–31 July 2023. WLG sites are listed from west to east in the legend. (a) TWL for C2 versus WLG, with 1:1 line shown for clarity, and regression statistics for a linear fit of the data. (b) Elevation difference between the WLG and C2 data with dots at the points of the C2 data and lines showing the location of the WLGs. The Newport and Weston sites are on the same longitude, but different latitude, and the dashed line represents this.

(Figure 1), as the water level ranges between low and high water over the 3-month period, the effects of coastal shallow water morphology can be assessed.

Comparisons between SWOT L3 and WLG for four individual sites can be seen in Figures 5–7, with the sites ordered going anticlockwise around the study region (Figure 1). The scatter plot and regression fits given in panel a) in Figures 5–7 and the Van de Casteele diagrams in panel b); outliers have not been excluded. In the Van de Casteele diagrams (Figures 5b–7b), points plotting left of the zero line of elevation difference show the gauge water level is greater than the altimeter water level. Scaling effects are seen at all the sites shown (e.g., Figures 5–7). This suggests distortion by shallow waters compared to the main channel (Fortunato & Oliveira, 2005; Friedrichs & Aubrey, 1988, 1994). The amplitude of the tidal curve increases substantially from west to east in the study area, so any small bias in location east-west between WLG and SWOT data points will inevitably result in a scaling error. Similar scaling effects have been seen when comparing GNSS-IR WLGs with standard gauges caused by tropospheric delays (Williams & Nievinski, 2017), which may be the result of the difficulty of modeling the wet tropospheric delay at the coast (Andersen & Scharroo, 2011). However, given the differences between sites in the study area and their location in respect to the main channel and intertidal areas, this scaling is assumed to be mainly due to differences in the coastal bathymetry.

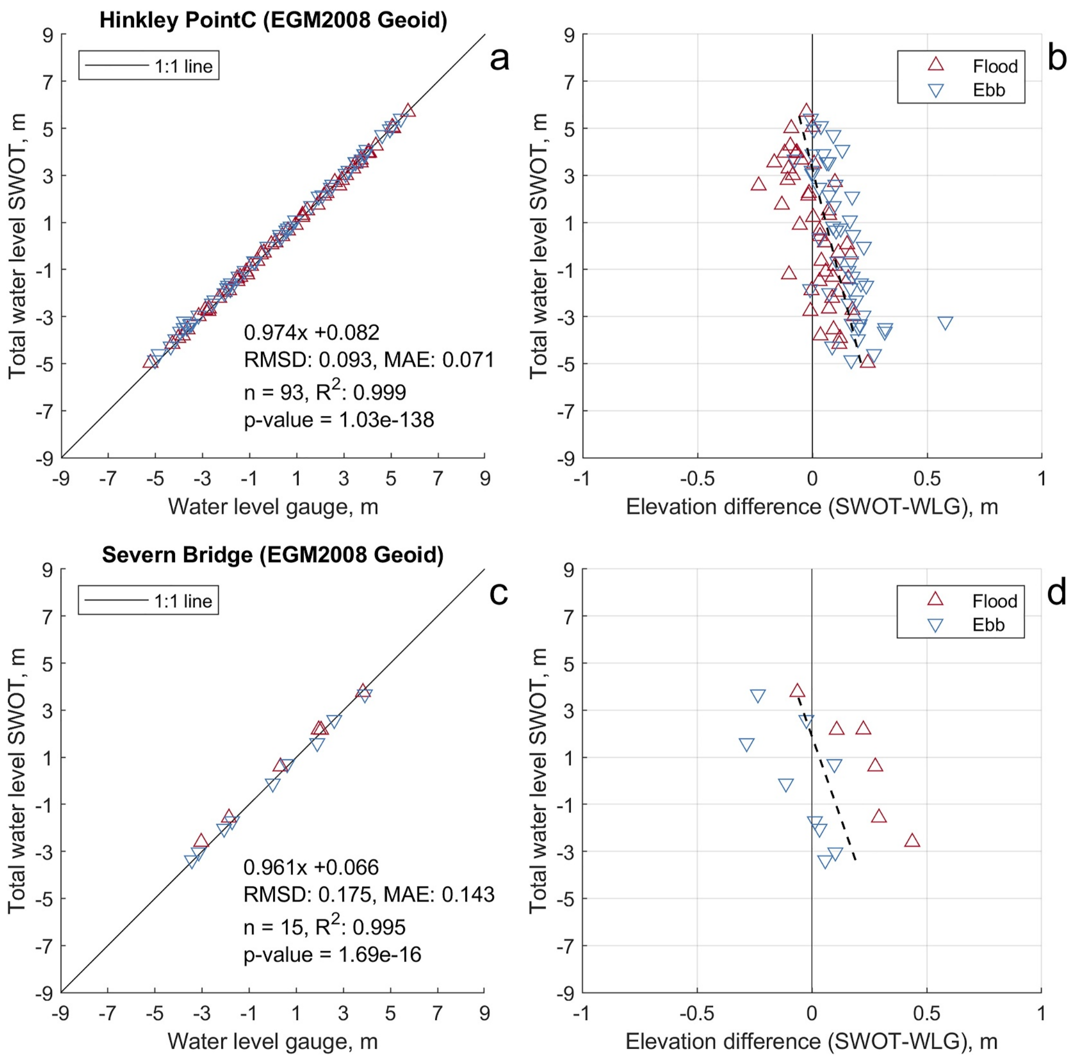

Figure 5. Surface water and ocean topography (SWOT) L3 LR Expert (v2.0.1) total water level (TWL) at Hinkley Point C (a and b) and Severn Bridge (c and d), median for the 6 km radius around the water level gauges, against WLG (corrected to EMG2008 geoid). (a, c) TWL for SWOT versus WLG, with 1:1 line shown for clarity, and regression statistics for a linear fit of the data. (b, d) Van de Casteele diagram, water elevation difference against water level, with a linear fit shown by the dashed line.

The Hinkley Point C gauge is installed on the end of a 460 m pier, allowing more uniform SWOT coverage around the site compared to land-based sites, and is away from major rivers. However, the slope in the Van de Casteele diagram shows there is a scaling effect and scatter due to difference between flood and ebb tide and at low water (Figure 5b). Severn Bridge, the furthest up estuary of the gauges in this study, is near intertidal areas and at the mouth of the River Severn (Figures 5c and 5d). The separation between flood and ebb tide can be clearly seen, forming a loop trajectory (Figure 5d). At Newport this effect of separation between flood and ebb with the height of tide is more evident for the lower part of the tide, −5 to 0 m (Figures 6b and 6d). The loss of data, due to problems in Level 1B processing, from L3 LR Expert v2.0.1 compared to L3 LR Expert v0.3 can be seen in Figure 6. For Nell's Point (Figure 7b), the ebb shows less scatter and a defined slope. However, there is greater overall scatter in the GNSS-IR data from Nell's Point (Figure 7) and Weston (not shown), as the measurement point changes between zones around the gauge as navigation satellites pass over and due to error from wind and wave effecting the sea roughness (Geremia-Nievinski et al., 2020; Larson et al., 2017; Löfgren & Haas, 2014). The higher elevation of the Nell's Point GNSS-IR causes more scatter due to this effect, as it samples a larger area, and water surface slope would have greater influence (Larson et al., 2017; Löfgren & Haas, 2014).

10.1029/2024EA004104

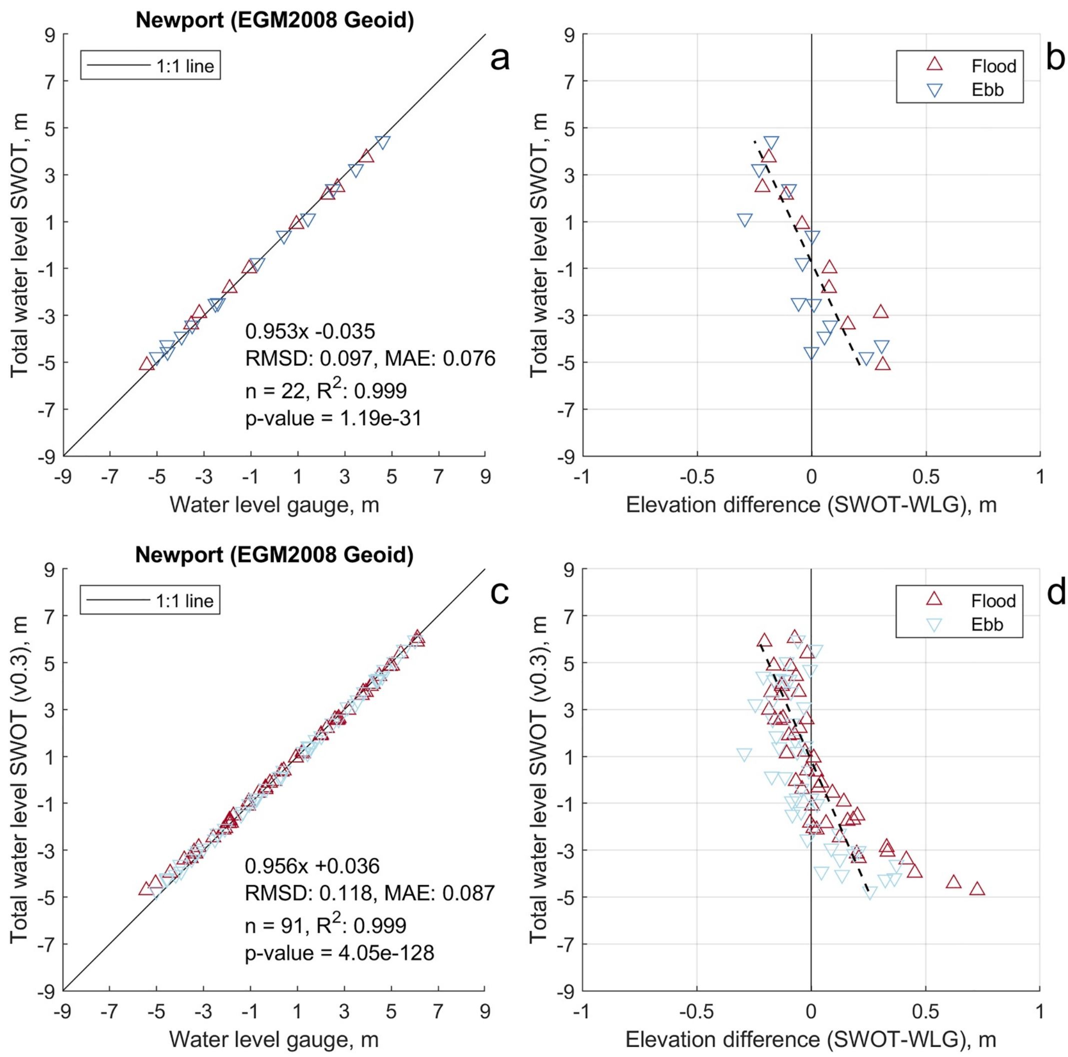

Figure 6. Surface water and ocean topography (SWOT) LR Expert total water level (TWL) at Newport, median for the 6 km radius around the water level gauges, against WLG (corrected to EMG2008 geoid). Panels a and b show the L3 LR Expert (v2.0.1) data, and panels c and d show the L3 LR Expert (v0.3) data. (a and c) TWL for SWOT versus WLG, with 1:1 line shown for clarity, and regression statistics for a linear fit of the data. (b and d) Van de Casteele diagram, water elevation difference against water level, with a linear fit shown by the dashed line.

3.5. SWOT L3 Comparison to Water Level Gauge Data

The SWOT L3 data were analyzed using data from the WLGs within the SWOT swath, shown in Figure 1, for the period 31 March–10 July 2023. Due to the effects of varying water level during ebb tide seen in the Van de Casteele diagrams (Section 3.4, above), the data from the ebb tide was excluded for the SWOT validation analysis. Outliers were identified by removing the scaling effect slope between SWOT water level and the water level difference and excluding points greater than three times the median absolute deviation.

Compared to the C2 analysis (Figure 4), the SWOT L3 LR Expert data are of similar quality with linear regression slope 0.966 and offset +0.049 m, RMSD 0.128 m and MAE 0.100 m, and R^2 0.998 (outliers excluded. Figure S2 Supporting Information S1). Removing the scaling effect slope, seen in the Van de Casteele diagrams, in the data from the individual sites (Pérez et al., 2014; Williams et al., 2020), gives a slope of 0.99 and offset +0.044 m, RMSD 0.137 m and MAE 0.106 m (Figure 8). Removing the scaling effect slope and offset from the individual sites, correcting for any differences in leveling and orbit bias as well as the scaling (Pérez et al., 2012), gives a regression slope 0.999 and offset +0.001 m, and RMSD 0.101 m and MAE 0.072 m (Figure S3 Supporting Information S1).

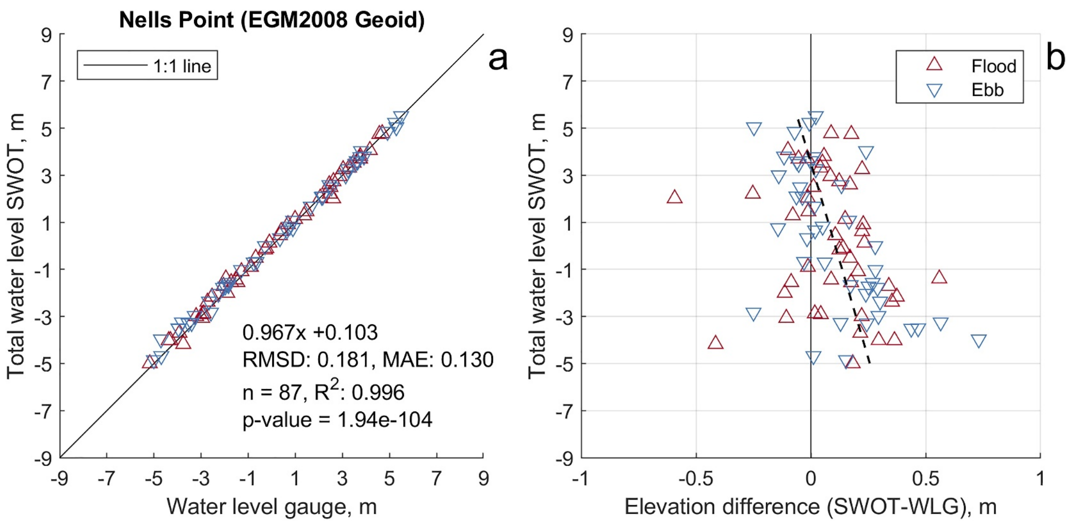

Figure 7. Surface water and ocean topography (SWOT) L3 LR Expert (v2.0.1) total water level (TWL) at Nell's Point (Global navigation satellite systems interferometric reflectometry system), median for the 6 km radius around the water level gauges, against WLG (corrected to EMG2008 geoid). (a) TWL for SWOT versus WLG, with 1:1 line shown for clarity, and regression statistics for a linear fit of the data. (b) Van de Casteele diagram, water elevation difference against water level, with a linear fit shown by the dashed line.

The site with the best fit was Penarth, with a scaling corrected fit slope of 0.999 and offset of +0.003 m, RMSD 0.059 m and MAE 0.041 m ($n = 17$. Figure S16 Supporting Information S1). Based on the regressions of the individual sites, corrected for scaling effect, an uncertainty in the range 0.059–0.150 m RMSD, 0.041–0.113 m MAE, was found for the SWOT L3 LR data (Figures S12–S18 Supporting Information S1).

4. Discussion

Making a qualitative spatial comparison of water level, using the FES2022 tidal model, shows SWOT KaRIn can resolve 2D features of the tidal elevation in the study area. Comparison with WLG data shows that the absolute measurements of the SWOT L3 LR Expert data have similar uncertainty to C2. The uncertainty of the SWOT L3 LR Expert data was further reduced by using only the flood tide data and correcting for the scaling slope with variation in water level. The 3-month cal/val data has allowed a comparison to the WLGs that shows the effects of nearshore processes on the individual gauges. This reveals the effect of shallow water morphology on the relationship between SWOT and WLG data, due to the spatial offset between the measurements. Once corrected for scaling slope, an uncertainty in the range 0.059–0.150 m RMSD, 0.041–0.113 m MAE, would be expected for individual SWOT L3 LR Expert (v2.0.1) SSH measurements in the coastal zone. Excluding the GNSS-IR gauges, which showed greater uncertainty (e.g., Nell's Point, Figure 7), the SWOT-WLG regression had an uncertainty of 0.102 m RMSD, 0.074 m MAE (Figure S4 Supporting Information S1). It should be noted that these values include the uncertainty of the water level gauges, as well as SWOT. This means that in the study area, the WLG network has an overall uncertainty of better than 0.102 m RMSD, 0.074 m MAE, and close to the 0.1 m uncertainty limit of the UK WLG network (Ordnance survey, 2023a). However, individual sites had less uncertainty, due to location, and this should be considered when selecting WLG sites for long-term studies.

Version 2.0.1 of the SWOT L3 LR Expert excludes some data in this study area. This reduced the number of points available for some of the sites. Newport and Avonmouth returned about 75% fewer points for the v2.0.1 product compared to v0.3. This is due to a problem with missing data in the reference surface used for the Level 1B processing, which is due to be corrected in the next Level 1B release version (SWOT Project, 2024).

Many water level gauges are located at seaports and harbors, which are often in locations sheltered from the open sea and located near river mouths for easy access to the hinterland by boat (Bradshaw et al., 2016; Cunliffe, 2001). This results in some gauge measurements being influenced by river flow and local coastal morphology when the altimeter measurements are less affected, as the altimeters cannot measure right at the coast. The data suggests that the coastal processes affect WLG readings more than the altimeter data at some sites, over the changing state

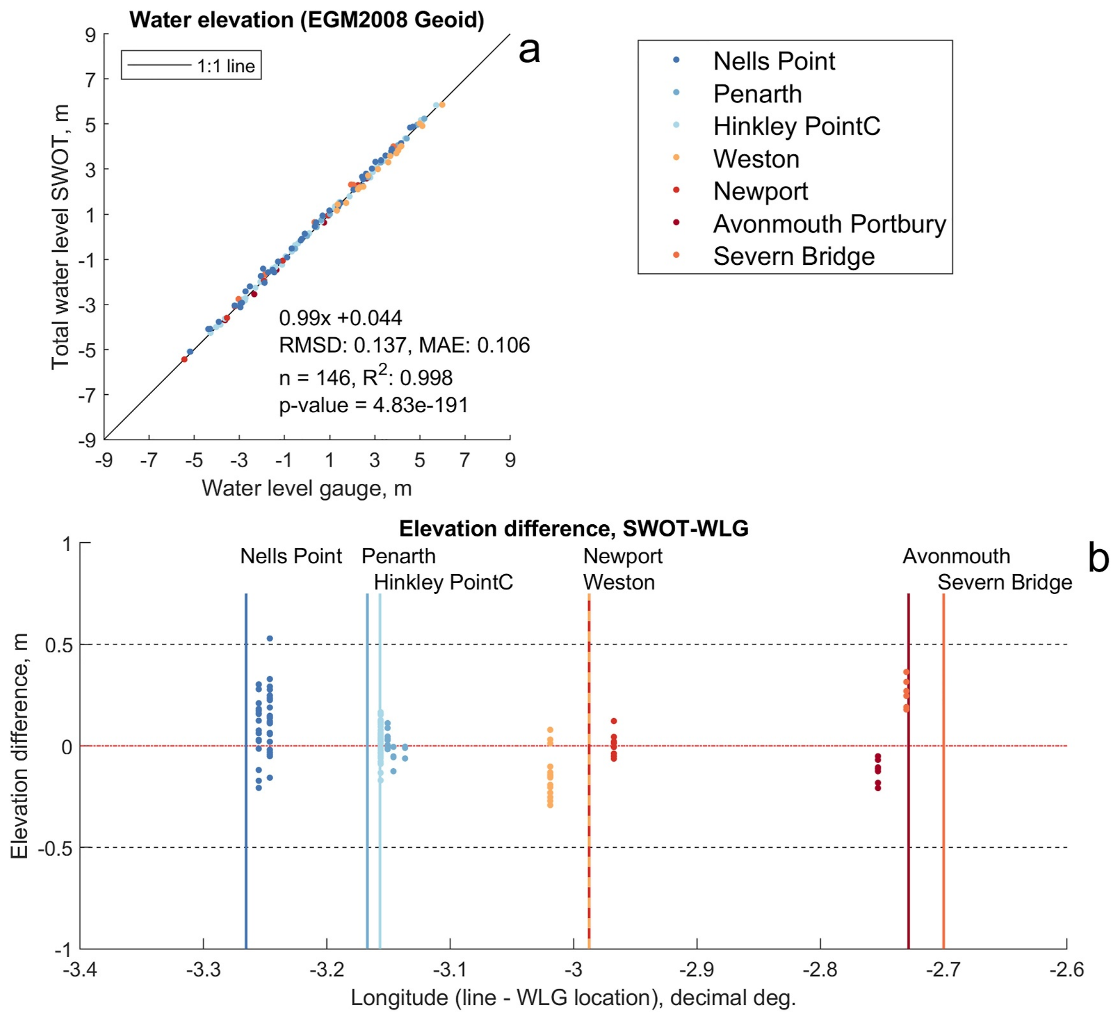

Figure 8. Surface water and ocean topography L3 LR Expert (v2.0.1) total water level (TWL), median for the 6 km radius around the water level gauges, against WLG (corrected to EMG2008 geoid). Data for March-July 2023. Flood tide only and outliers filtered for the effects of shallow water. Data are corrected for scaling effect with water elevation. WLG sites are listed from west to east in the legend (ordered by longitude). (a) TWL for L3 versus WLG, with 1:1 line shown for clarity, and regression statistics for a linear fit of the data. (b) Elevation difference between the WLG and L3 data with dots at the points of the L3 data and lines showing the location of the WLGs. The Newport and Weston sites are on the same longitude, but different latitude, and the dashed line represents this.

of tide, with intertidal areas causing clear differences between flood and ebb tide (e.g., Severn Bridge and Newport, Figures 5 and 6).

Initially, it was assumed that the WLG network was accurate enough overall to validate the altimetry data, but some of the individual gauges showed high uncertainty in the scatter of the data. Intertidal morphology (flats and banks) will affect the flow of water and amplitude of the tide. The scaling of the water level data, for example, Figure 6b, due to the location of the WLG and separation from the point of altimeter measurement shows that care is needed when using coastal gauges. Plotting the Van de Casteele diagram for each WLG was essential to understanding these problems. It is recommended that data are selected from the flood or ebb tide for validating altimetry data using coastal WLGs, and corrected for the scaling slope and offset, depending on local shallow water effects. Spikes and artifacts in the satellite data mean that single points cannot always be trusted in isolation. Over multiple passes uncertainty can be reduced. Overall, the altimetry data set shows good agreement with the WLG network, once the limitations of individual sites are accounted for.

The orbit of C2 results in tracks intersecting with the coastline near to perpendicular and scattering either side of the WLGs. The SWOT KaRIn data also scatters around WLG locations. Using the median value of SWOT data reduces the effect of channel slope for different states of tide over the period of data collection. However, this could possibly be better corrected using statistical methods, such as Kriging, to extrapolate the altimetry measurements to the point of the WLGs. Nearshore effects of wave set up and set down are more difficult to account for as they occur over short length scales, too close to shore to be resolved.

For C2's ∼369 days repeat cycle, in 10 years of data there should be 10 or more passes for each track. However, for the 1 Hz data, due to gaps in the corrections and spacing between the samples, the number of points returned is much lower. The quality control applied to the C2 data used can also remove too much data, as the process is tuned for ocean altimetry.

Uncertainty in the gauge data due to river flow could be reduced in the validation using river level data from further upstream, where available. As this is a complicated process, gauges with measurement values clearly influenced by the river flow, with all the points scattered below the one-to-one line, were excluded from the validation analysis.

The water surface slope represents error in the matching of the SWOT data to WLG. In the Bristol Channel, where the tide circulates as a Kelvin wave, the cross-channel slope will have an effect, less so for the Severn Estuary as it narrower. The mean along channel slope was found to be about twice that of the cross-channel slope. A range of extrapolation methods were tested on the SWOT L3 data, to estimate the water level at the locations of the WLGs. These included linear and cubic extrapolation, and different types of Kriging (including accounting for anisotropy due to the angle of the main channel), the median still was best with regression kriging (correcting for anisotropy) a very close second when comparing the RMSD. This is probably due to the median working well for the along channel slope and the extrapolation methods not accounting for nearshore processes cross-channel/cross-shore. The near-shore bathymetry and morphology affect the measurements of the WLGs (set down and set up), and the cross and along channel slope cannot correct for all the uncertainty between the satellite and WLG measurements. The Van de Casteele slope correction attempts to correct for the differences between the satellite and WLG measurements, however, for some sites the relationship is non-linear, and this could be improved with future work.

The Van de Casteele plots for the GNSS-IR gauges show greater scatter than the standard WLGs. This is because GNSS-IR water level measurements are inherently noisier than traditional WLGs (Geremia-Nievinski et al., 2020; Larson et el., 2017). Reasons include time varying surface effects, tropospheric delay, roughness of the water surface, multipath not related to the water surface, aggregation time of the measurements and changes in sampling locations.

Systematic errors will always be a source of uncertainty and the crossover correction, reducing these effects, is expected to improve with newer processing versions. As the SWOT wave products improve, the SSB correction is also expected to improve.

The removal of individual values by filtering the data impacts on the temporal frequency of the data, however for this evaluation it was more important to measure as much of the tidal range as possible, at different states of tide, to get a good relationship. These data cover about eight spring-neap tidal cycles and, across all the sites, almost the full spring-neap tidal range is covered. In addition, the daily repeat data of the cal/val phase provides much higher temporal frequency than the operational science orbit. For this work, the 3-month daily repeat phase is equivalent to about 3 years of data from the science orbit, as there is a swath cross-over in the study area. For areas not covered by a swath cross-over, it would take about 5.6 years to measure the same number of passes. This highlights the key benefit of the daily repeat cal/val phase, in that it builds up a large data set over a short period of time.

Daily data are only available for the 3-month period of the cal/val phase. Although these data provide a unique opportunity for studying coastal processes, the 21-repeat Science orbit provides the ongoing operational data. Though this orbit repeat is much less frequent, missing coastal changes on a daily to week time scale, the global coverage opens the opportunity to study a wider range of sites dominated by different processes. In addition, with higher latitude the number swath crossovers increase, which gives a more frequent revisit time. Oceanographic features that move from east to west, with the progression of SWOT's science orbit, at the scale of the swath could be tracked over successive daily swaths (such as storm surges).

Future work aims to compare the SWOT KaRIn water levels to a new 500 m resolution NEMO model for the UK region, to Sentinel-1 data using the temporal waterline method for intertidal elevations, and to the UK operational storm surge model.

5. Conclusions

Here a comparison was made of SWOT L3 LR Expert SSH 2 km data v2.0.1 (Baseline C) data with measurements from the UK WLG network, in the coastal region of the BCSRE. Plotting the Van de Casteele diagram, of variation of difference between altimeter and WLG with water elevation, for each WLG was essential to understanding the effect of nearshore processes when comparing distance between WLG and the point of altimeter measurement. Once corrected for scaling effect with water elevation, seen in the Van de Casteele diagrams, the regressions for the individual sites had an uncertainty of 0.059–0.150 m RMSD, 0.041–0.113 m MAE. For all the sites combined the regression had a slope of 0.99 and offset +0.044, RMSD 0.137 m and MAE 0.106 m. Given the uncertainties, from the various sources detailed above (Section 1.5), this shows that SWOT is returning high quality data in this challenging environment.

A qualitative spatial comparison of water level shows SWOT is resolving the expected tidal patterns. In addition, SWOT has the potential to measure intertidal areas for the study of coastal morphology and habitat.

Looking at the WLG network using the C2 and SWOT data, the WLGs are consistent over the area. Although the sites are affected by the nearshore environment, this uncertainty in collocation can be reduced using the Van de Casteele diagrams to determine a correction. Compared with SWOT, an overall uncertainty of better than 0.102 m RMSD, 0.074 m MAE, is expected for the WLG network in the study area (excluding the GNSS-IR sites).

There are potentially significant amounts of information on spatial variability in the coastal zone from standard altimetry data, but it is unused due to issues like flagging, SSB inaccuracies and problems with model corrections at the land-sea boundary. The 1-day repeat orbit phase of the SWOT commissioning process has allowed the high-frequency collection of a high-quality validation data set. These data have the potential to resolve coastal processes, such as river discharge events, movement of sandbanks and storm surges, which would be missed in the 21-day repeat data.

Conflict of Interest

The authors declare no conflicts of interest relevant to this study.

Data Availability Statement

The SWOT data products are produced and made freely available by the joint SWOT (NASA/JPL and CNES) project. The product quality is not final and will be affected by some evolutions as the SWOT project team makes progress on science data processing algorithms and instrument calibrations. The SWOT_L3_LR_SSH product, derived from the L2 SWOT KaRIn low-rate ocean data products (L2_LR_SSH) (NASA/JPL and CNES), is produced and made freely available by AVISO and DUACS teams as part of the DESMOS Science Team project. AVISO/DUACS, 2024. SWOT Level 3 SSH Expert (v2.0.1) [Dataset]. CNES. https://doi.org/10.24400/527896/A01-2023.018 (AVISO, 2024b, 2024c). The C2 data were downloaded from ftp://science-pds.cryosat.esa.int/, see https://earth.esa.int/eogateway/catalog/cryosat-products for details (European Space Agency, 2024). The WLG data are from the Environment Agency Real Time flood-monitoring API and the Regional Coastal Monitoring Programme (CCO API), made freely available under the terms of the Open Government License. Please note that these are real-time data and are not quality controlled. Additional archive data were supplied by the EA, on request. Contains public sector information licensed under the Open Government License v3.0. The WLG data used for this paper are archived at the British Oceanographic Data Centre, https://www.bodc.ac.uk/data/published_data_library/catalogue/10.5285/25129f9a-7369-9ab2-e063-7086abc05905 (Lichtman et al., 2024). The FES2022 Tide product was funded by CNES, produced by LEGOS, NOVELTIS and CLS and made freely available by AVISO." CNES, 2024. FES2022 (Finite Element Solution) Ocean Tide (Version 2022) [Dataset]. CNES. https://doi.org/10.24400/527896/A01-2024.004. The analysis and plotting were carried out in MATLAB and the code is accessible in Zenodo, 10.5281/zenodo.13969266 (Lichtman & Bell, 2024) geographiclib was written by Charles Karney (2024) and is available at https://www.mathworks.com/matlabcentral/fileexchange/50605-geographiclib, MATLAB

Central File Exchange. (Accessed 16 October 2024). The existfield function was created from a post by Bill Connelly (30 October 2015), Matlab answers: Is there a MATLAB function that can check if a field exists in a MATLAB structure? https://uk.mathworks.com/matlabcentral/answers/95923-is-there-a-matlab-function-that-can-check-if-a-field-exists-in-a-matlab-structure.

Acknowledgments
The SWOT-UK project was funded by the United Kingdom Natural Environment Research Council and the United Kingdom Space Agency (SWOT Cal/Val AO), under Grant NE/V009168/1. Thanks to Chris Balfour and Richard Cooke at the NOC for the construction and deployment of the GNSS-IR system at Clevedon Pier, and to Paul Bates and Jeff Neal from the University of Bristol for their assistance with the installations. We would also like to express our thanks to the hosts of the three GNSS-IR gauges deployed for the project at The National Coastwatch Institution lookout station at Nells Point near Barry, South Wales, and at Grand Pier, Weston-Super-Mare, and Clevedon Pier. Additional thanks to the Environment Agency, Channel Coastal Observatory and Vale of Glamorgan Council for additional information on the tidal gauge network, and to Gwyn Nelson at the Welsh Coastal Monitoring Centre for support with surveying in the GNSS-IR gauge at Nells Point. The color maps used for the graphs are from colorbrewer2.org (Harrower & Brewer, 2003).

References

Abessolo, G. O., Birol, F., Almar, R., Léger, F., Bergsma, E., Brodie, K., & Holman, R. (2023). Wave influence on altimetry sea level at the coast. *Coastal Engineering*, *180*, 104275. https://doi.org/10.1016/j.coastaleng.2022.104275

Akima, H. (1970). A new method of interpolation and smooth curve fitting based on local procedures. *Journal of the ACM*, *17*(4), 589–602. https://doi.org/10.1145/321607.321609

Andersen, O. B., & Scharroo, R. (2011). Range and geophysical corrections in coastal regions: And implications for Mean Sea Surface determination. In S. Vignudelli, A. Kostianoy, P. Cipollini, & J. Benveniste (Eds.), *Coastal altimetry*. Springer. https://doi.org/10.1007/978-3-642-12796-0_5

Archer, A. W. (2013). World's highest tides: Hypertidal coastal systems in North America, South America and Europe. *Sedimentary Geology*, *284–285*, 1–25. https://doi.org/10.1016/j.sedgeo.2012.12.007

AVISO. (2024a). SWOT orbit. Retrieved from https://www.aviso.altimetry.fr/en/missions/current-missions/swot/orbit.html

AVISO. (2024b). SWOT_L2_KaRIn_SSH_Expert product. https://doi.org/10.24400/527896/a01-2023.015

AVISO. (2024c). SWOT_L3_LR_SSH_Expert product. https://doi.org/10.24400/527896/A01-2023.018

AVISO. (2024d). FES2022 (finite element solution) Ocean Tide product handbook. *SALP-MU-P-EA-23561-CLS, issue 1, rev 0*. https://doi.org/10.24400/527896/a01-2024.004

AVISO. (2025). DUACS level-3 SWOT KaRIn (L3_LR_SSH) user handbook. issue 1.5. Retrieved from https://www.aviso.altimetry.fr/fileadmin/documents/data/tools/hdbk_duacs_SWOT_L3.pdf

Blewitt, G., Kreemer, C., Hammond, W. C., & Gazeaux, J. (2016). MIDAS robust trend estimator for accurate GPS station velocities without step detection. *Journal of Geophysical Research: Solid Earth*, *121*(3), 2054–2068. https://doi.org/10.1002/2015JB012552

Bonnefond, P., Haines, B. J., & Watson, C. (2011). In situ absolute calibration and validation: A link from coastal to open-ocean altimetry. In S. Vignudelli, A. Kostianoy, P. Cipollini, & J. Benveniste (Eds.), *Coastal altimetry*. Springer. https://doi.org/10.1007/978-3-642-12796-0_11

Bradshaw, E., Woodworth, P. L., Hibbert, A., Bradley, L. J., Pugh, D. T., Fane, C., & Bingley, R. M. (2016). A century of Sea Level measurements at Newlyn, Southwest England. *Marine Geodesy*, *39*(2), 115–140. https://doi.org/10.1080/01490419.2015.1121175

Calafat, F. M., Cipollini, P., Bouffard, J., Snaith, H., & Féménias, P. (2017). Evaluation of new CryoSat-2 products over the ocean. *Remote Sensing of Environment*, *191*, 131–144. https://doi.org/10.1016/j.rse.2017.01.009

Carling, P. A., Radecki-Pawlik, A., Williams, J. J., Rumble, B., Meshkova, L., Bell, P., & Breakspear, R. (2006). The morphodynamics and internal structure of intertidal fine-gravel dunes: Hills Flats, Severn Estuary, UK. *Sedimentary Geology*, *183*(3–4), 159–179. https://doi.org/10.1016/j.sedgeo.2005.07.007

Cazenave, A., Gouzenes, Y., Birol, F., Leger, F., Passaro, M., Calafat, F. M., et al. (2022). Sea level along the world's coastlines can be measured by a network of virtual altimetry stations. *Communications Earth & Environment*, *3*(1), 117. https://doi.org/10.1038/s43247-022-00448-z

Channel Coastal Observatory. (2024). CCO API v1.1 developer information [Online]. Retrieved from https://coastalmonitoring.org/ccoresources/api/

Cipollini, P., Calafat, F. M., Jevrejeva, S., Melet, A., & Prandi, P. (2017). Monitoring Sea level in the coastal zone with satellite altimetry and tide gauges. *Surveys in Geophysics*, *38*(1), 33–57. https://doi.org/10.1007/s10712-016-9392-0

Cunliffe, B. W. (2001). *Facing the ocean: The atlantic and its peoples, 8000 BC-ad 1500*. Oxford University Press.600

Dhoop, T. (2019). Coastal wave network annual report 2018. Channel coastal observatory. Retrieved from https://www.coastalmonitoring.org/reports/

Dibarboure, G., Ubelmann, C., Flamant, B., Briol, F., Peral, E., Bracher, G., et al. (2022). Data-driven calibration algorithm and pre-launch performance simulations for the SWOT mission. *Remote Sensing*, *14*(23), 6070. https://doi.org/10.3390/rs14236070

Dow, J. M., Neilan, R. E., & Rizos, C. (2009). The international GNSS service in a changing landscape of global navigation satellite systems. *Journal of Geodesy*, *83*(7), 191–198. https://doi.org/10.1007/s00190-009-0315-4

Dyer, K. R. (1984). Sedimentation processes in the Bristol Channel/Severn estuary. *Marine Pollution Bulletin*, *15*(2), 53–57. https://doi.org/10.1016/0025-326x(84)90462-4

Environment Agency. (2024). Environment agency real time flood-monitoring API [Online]. Retrieved from https://environment.data.gov.uk/flood-monitoring/doc/reference

Esteban-Fernandez, D. E. (2017). SWOT project mission performance and error budget, Revision A. Retrieved from https://swot.jpl.nasa.gov/system/documents/files/2178_2178_SWOT_D-79084_v10Y_FINAL_REVA__06082017.pdf

European Space Agency. (2021). CryoSat-2 product handbook Baseline-E 1.0, draft C. C2-LI-ACS-ESL-5319 [Online]. Retrieved from https://earth.esa.int/eogateway/documents/20142/0/CryoSat-Product-Handbook-Baseline-E-draft.pdf

European Space Agency. (2024). Earth online EO gateway: CryoSat-2 products [Online]. Retrieved from https://earth.esa.int/eogateway/catalog/cryosat-products

Falconer, R. A., Xia, J. Q., Lin, B. J., & Ahmadian, R. (2009). The Severn barrage and other tidal energy options: Hydrodynamic and power output modelling. *Science in China Series E: Technological Sciences*, *52*(11), 3413–3424. https://doi.org/10.1007/s11431-009-0366-z

Fortunato, A., & Oliveira, A. (2005). Influence of intertidal flats on tidal asymmetry. *Journal of Coastal Research*, *21*(5), 1062–1067. https://doi.org/10.2112/03-0089.1

Friedrichs, C. T., & Aubrey, D. G. (1988). Non-linear tidal distortion in shallow well-mixed estuaries: A synthesis. *Estuarine, Coastal and Shelf Science*, *27*(5), 521–545. https://doi.org/10.1016/0272-7714(88)90082-0

Friedrichs, C. T., & Aubrey, D. G. (1994). Tidal propagation in strongly convergent channels. *Journal of Geophysical Research*, *99*(C2), 3321–3336. https://doi.org/10.1029/93jc03219

Fu, L.-L., Alsdorf, D., Rodriguez, E., Morrow, R., Mognard, N., Lambin, J., et al. (2009). The SWOT (surface water and Ocean Topography) mission: Spaceborne radar interferometry for oceanographic and hydrological applications. In *Proceedings of the OCEANOBS'09 conference (Venice-Lido)*. Venice-Lido.

Fu, L.-L., Pavelsky, T., Cretaux, J.-F., Morrow, R., Farrar, J. T., Vaze, P., et al. (2024). The surface water and Ocean Topography mission: A breakthrough in radar remote sensing of the ocean and land surface water. *Geophysical Research Letters*, *51*(4), e2023GL107652. https://doi.org/10.1029/2023GL107652

Gao, C., & Adcock, T. A. A. (2017). On the tidal resonance of the Bristol Channel. *International Journal of Offshore and Polar Engineering*, *27*(2), 177–183. https://doi.org/10.17736/ijope.2017.as19

Geremia-Nievinski, F., Hobiger, T., Haas, R., Liu, W., Strandberg, J., Tabibi, S., et al. (2020). SNR-Based GNSS reflectometry for coastal sea-level altimetry: Results from the first IAG inter-comparison campaign. *Journal of Geodesy*, *94*(70), 70. https://doi.org/10.1007/s00190-020-01387-3

Gravelle, M., Wöppelmann, G., Gobron, K., Altamimi, Z., Guichard, M., Herring, T., & Rebischung, P. (2023). The ULR-repro3 GPS data reanalysis and its estimates of vertical land motion at tide gauges for sea level science. *Earth System Science Data*, *15*(1), 497–509. https://doi.org/10.5194/essd-15-497-2023

Gregg, D. E., Penna, N. T., Jones, C., & Morales Maqueda, M. A. (2024). Accuracy assessment of recent global ocean tide models in coastal waters of the European North West Shelf. *Ocean Modelling*, *192*, 102448. https://doi.org/10.1016/j.ocemod.2024.102448

Hammond, W. C., Blewitt, G., Kreemer, C., & Nerem, R. S. (2021). GPS Imaging of global vertical land motion for studies of sea level rise. *Journal of Geophysical Research: Solid Earth*, *126*(7), e2021JB022355. https://doi.org/10.1029/2021JB022355

Harrower, M., & Brewer, C. A. (2003). ColorBrewer.org: An online tool for selecting colour schemes for maps. *The Cartographic Journal*, *40*(1), 27–37. https://doi.org/10.1179/000870403235002042

Hart-Davis, M. G., Andersen, O. B., Ray, R. D., Zaron, E. D., Schwatke, C., Arildsen, R. L., et al. (2024). Tides in complex coastal regions: Early case studies from wide-swath SWOT measurements. *Geophysical Research Letters*, *51*(20), e2024GL109983. https://doi.org/10.1029/2024GL109983

Horsburgh, K., & Horritt, M. (2006). The Bristol Channel floods of 1607—Reconstruction and analysis. *Weather*, *61*(10), 272–277. https://doi.org/10.1256/wea.133.05

IOC. (1985). Manual on sea-level measurement and interpretation. Volume I: Basic procedures. *Intergovernmental Oceanographic Commission, Manuals & Guides*, *14*, 84.

Ionita, A. C. (2019). Cleve's corner: Cleve moler on mathematics and computing. *Makima Piecewise Cubic Interpolation [Blog]*. Retrieved from https://blogs.mathworks.com/cleve/2019/04/29/makima-piecewise-cubic-interpolation/

JPL. (2023). SWOT product description document: Level 2 KaRIn low rate Sea Surface height (L2_LR_SSH) data product. *Jet Propulsion Laboratory Internal Document, D-56407, Revision B*.

Karney, C. F. F. (2013). Algorithms for geodesics. *Journal of Geodesy*, *87*(1), 43–55. https://doi.org/10.1007/s00190-012-0578-z

Laignel, B., Ayoub, N., Birol, F., Brown, S., Chao, Y., Cornuelle, B., et al. (2015). Coastal and Estuaries White Paper. Part 1: Estuaries and nearshore processes Issues and SWOT contribution in the coastal zones and estuaries. Retrieved from https://www.aviso.altimetry.fr/fileadmin/documents/missions/Swot/WhitePaperSWOTCoastEstuary_Part1.pdf

Laignel, B., Vignudelli, S., Almar, R., Becker, M., Bentamy, A., Benveniste, J., et al. (2023). Observation of the coastal areas, estuaries and deltas from Space. *Surveys in Geophysics*, *44*(5), 1309–1356. https://doi.org/10.1007/s10712-022-09757-6

Larson, K. M., Ray, R. D., & Williams, S. D. P. (2017). A 10-year comparison of water levels measured with a geodetic GPS receiver versus a conventional tide gauge. *Journal of Atmospheric and Oceanic Technology*, *34*(2), 295–307. https://doi.org/10.1175/JTECH-D-16-0101.1

Lichtman, I. D., & Bell, P. S. (2024). Analysis and plotting software for evaluating water levels from the Surface Water and Ocean Topography (SWOT) mission in a coastal and estuarine environment (Bristol Channel-Severn Estuary) using water level gauges (1.0). Software. *Zenodo*. https://doi.org/10.5281/zenodo.13969266

Lichtman, I. D., Bell, P. S., Williams, S. D. P., Gommenginger, C., Banks, C., Calafat, F. M., & Brown, J. (2024). Water level data from the Bristol Channel and Severn Estuary and River region for validation of satellite altimeters, 2012-2023 (SWOT-UK project) [Dataset]. *NERC EDS British Oceanographic Data Centre NOC*. https://doi.org/10.5285/25129f9a-7369-9ab2-e063-7086abc05905

Löfgren, J. S., & Haas, R. (2014). Sea level measurements using multi-frequency GPS and GLONASS observations. *EURASIP Journal on Applied Signal Processing*, *50*. https://doi.org/10.1186/1687-6180-2014-50

Lyddon, C., Brown, J. M., Leonardi, N., & Plater, A. J. (2018). Flood hazard assessment for a hyper-tidal estuary as a function of tide-surge-morphology interaction. *Estuaries and Coasts*, *41*(6), 1565–1586. https://doi.org/10.1007/s12237-018-0384-9

Lyddon, C., Brown, J. M., Leonardi, N., Saulter, A., & Plater, A. J. (2020). Quantification of the uncertainty in coastal storm hazard predictions due to wave-current interaction and wind forcing. *Geophysical Research Letters*, *46*(24), 14576–14585. https://doi.org/10.1029/2019GL086123

Lyddon, C., Robins, P., Lewis, M., Barkwith, A., Vasilopoulos, G., Haigh, I., & Coulthard, T. (2023). Historic spatial patterns of storm-driven compound events in UK estuaries. *Estuaries and Coasts*, *46*(1), 30–56. https://doi.org/10.1007/s12237-022-01115-4

Martín Míguez, B., Testut, L., & Wöppelmann, G. (2008). The Van de Casteele test revisited: An efficient approach to tide gauge error characterization. *Journal of Atmospheric and Oceanic Technology*, *25*(7), 1238–1244. https://doi.org/10.1175/2007JTECHO554.1

MathWorks, Inc. (2022). MATLAB help pages: Makima - modified Akima piecewise cubic hermite interpolation. Retrieved from https://uk.mathworks.com/help/matlab/ref/makima.html

Mertz, F., Dumont, J. P., & Urien, S. (2019). Baseline-C CryoSat ocean processor Ocean Product handbook. Version 4.1 [Online]. Retrieved from https://earth.esa.int/eogateway/documents/20142/37627/CryoSat-Baseline-C-Ocean-Product-Handbook.pdf/d4718bd4-65ae-20a6-5ea9-ee3cde121f7c

Michell, P. F. (2015). GridInQuest II coordinate transformation utility software. Version 1.01 [Computer program]. *Michell Computing*. Retrieved from https://bitbucket.org/PaulFMichell/gridinquestii/src/master/

Monahan, T., Tang, T., Roberts, S., & Adcock, T. A. A. (2025a). Observations of the seiche that shook the world. *Nature Communications*, *16*, 4777. https://doi.org/10.1038/s41467-025-59851-7

Monahan, T., Tang, T., Roberts, S., & Adcock, T. A. A. (2025b). Tidal corrections from and for SWOT using a spatially coherent variational Bayesian harmonic analysis. *Journal of Geophysical Research: Oceans*, *130*(3), e2024JC021533. https://doi.org/10.1029/2024JC021533

National Tidal and Sea Level Facility. (2024a). Avonmouth tide gauge site. Retrieved from https://ntslf.org/tgi/portinfo?port=Avonmouth

National Tidal and Sea Level Facility. (2024b). Hourly Residual Elevations–April 2023–Avonmouth. Retrieved from https://ntslf.org/files/surgemonthlyplots/202304/avon202304.pdf

National Tidal and Sea Level Facility. (2024c). Skew surge history: England–South. Retrieved from https://ntslf.org/storm-surges/skew-surges/england-south

Natural Resources Wales. (1996). Site of special scientific interest citation: River Wye. Retrieved from https://naturalresources.wales/media/663017/SSSI_1342_Citation_EN00132f4.pdf

Office for National Statistics. (2023). Digital boundaries. Licensed under the open government licence v.3.0. *Contains OS data © Crown copyright and database right*. Retrieved from https://www.ons.gov.uk/methodology/geography/geographicalproducts/digitalboundaries

Ordnance survey. (2023a). Accuracy of OS net. *OSTN15 and OSGM15*. Retrieved from https://www.ordnancesurvey.co.uk/business-government/tools-support/os-net/accuracy

Ordnance survey. (2023b). OSTN15 OSGM15 transformation software. Retrieved from https://www.ordnancesurvey.co.uk/business-government/tools-support/os-net/transformation

Pavlis, N. K., Holmes, S. A., Kenyon, S. C., & Factor, J. K. (2012). The development and evaluation of the earth gravitational model 2008 (EGM2008). *Journal of Geophysical Research*, *117*(B4), B04406. https://doi.org/10.1029/2011JB008916

Pérez, B., Payo, A., López, D., Woodworth, P. L., & Alvarez Fanjul, E. (2012). Overlapping sea level time series measured using different technologies: An example from the REDMAR Spanish network. *Natural Hazards and Earth System Sciences*, *14*, 589–610. https://doi.org/10.5194/nhess-14-589-2014

Ray, R. D., Egbert, G. D., & Erofeeva, S. Y. (2011). Tide predictions in shelf and coastal waters: Status and prospects. In S. Vignudelli, A. Kostianoy, P. Cipollini, & J. Benveniste (Eds.), *Coastal altimetry*. Springer. https://doi.org/10.1007/978-3-642-12796-0_8

Risk Management Solutions. (2007). 1607 Bristol Channel floods: 400-Year retrospective. *RMS special report*. Retrieved from https://forms2.rms.com/rs/729-DJX-565/images/fl_1607_bristol_channel_floods.pdf

Rulent, J., Bricheno, L. M., Green, J. A. M., Haigh, I. D., & Lewis, H. (2021). Distribution of coastal high water level during extreme events around the UK and Irish coasts. *Natural Hazards and Earth System Sciences*, *21*(11), 3339–3351. https://doi.org/10.5194/nhess-21-3339-2021

Rulent, J., Calafat, F. M., Banks, C. J., Bricheno, L. M., Gommenginger, C., Green, J. A. M., et al. (2020). Comparing water level estimation in coastal and shelf seas from satellite altimetry and numerical models. *Frontiers in Marine Science*, *7*, 549467. https://doi.org/10.3389/fmars.2020.549467

SONEL. (2023). Map of GNSS stations. Retrieved from https://www.sonel.org/-GPS-.html

Surface Water and Ocean Topography (SWOT) Project. (2024). Release note: SWOT version C KaRIn science data products. Retrieved from https://podaac-www.jpl.nasa.gov/announcements/2024-03-06-SWOT-KaRIn-Science-Data-Products-Release

SWOT AdAC Consortium. (2025). SWOT adopt-A-crossover (AdAC) Consortium [Online]. Retrieved from https://www.swot-adac.org/

Uncles, R. J. (1984). Hydrodynamics of the Bristol Channel. *Marine Pollution Bulletin*, *15*(2), 47–53. https://doi.org/10.1016/0025-326x(84)90461-2

Uncles, R. J. (2010). Physical properties and processes in the Bristol Channel and severn estuary. *Marine Pollution Bulletin*, *61*(1–3), 5–20. https://doi.org/10.1016/j.marpolbul.2009.12.010

Vignudelli, S., Birol, F., Benveniste, J., Fu, L.-L., Picot, N., Raynal, M., & Roinard, H. (2019). Satellite altimetry measurements of Sea Level in the coastal zone. *Surveys in Geophysics*, *40*(6), 1319–1349. https://doi.org/10.1007/s10712-019-09569-1

Williams, S. D. P., Bell, P. S., McCann, D. L., Cooke, R., & Sams, C. (2020). Demonstrating the potential of low-cost GPS units for the remote measurement of tides and water levels using interferometric reflectometry. *Journal of Atmospheric and Oceanic Technology*, *37*(10), 1925–1935. https://doi.org/10.1175/JTECH-D-20-0063.1

Williams, S. D. P., & Nievinski, F. G. (2017). Tropospheric delays in ground-based GNSS multipath reflectometry–Experimental evidence from coastal sites. *Journal of Geophysical Research: Solid Earth*, *122*(3), 2310–2327. https://doi.org/10.1002/2016JB013612

Woodworth, P. L., Melet, A., Marcos, M., Ray, R. D., Wöppelmann, G., Sasaki, Y. N., et al. (2019). Forcing factors affecting Sea Level changes at the coast. *Surveys in Geophysics*, *40*(6), 1351–1397. https://doi.org/10.1007/s10712-019-09531-1

Wöppelmann, G., & Marcos, M. (2016). Vertical land motion as a key to understanding sea level change and variability. *Reviews of Geophysics*, *54*(1), 64–92. https://doi.org/10.1002/2015RG000502